Effect of skin hydration on the dynamics of fingertip gripping contact

T. André[1,2], V. Lévesque[3], V. Hayward[4], P. Lefèvre[1,2] and J.-L. Thonnard[1,*]

[1] *Institute of Neuroscience (IoNS), Université catholique de Louvain, Brussels, Belgium*
[2] *Institute of Information and Communication Technologies, Electronics and Applied Mathematics (ICTEAM), Université catholique de Louvain, Louvain-la-Neuve, Belgium*
[3] *Department of Computer Science, University of British Columbia, Vancouver, Canada*
[4] *UPMC Univ Paris 06, Institut des Systèmes Intelligents et de Robotique, 75005 Paris, France*

The dynamics of fingertip contact manifest themselves in the complex skin movements observed during the transition from a stuck state to a fully developed slip. While investigating this transition, we found that it depended on skin hydration. To quantify this dependency, we asked subjects to slide their index fingertip on a glass surface while keeping the normal component of the interaction force constant with the help of visual feedback. Skin deformation inside the contact region was imaged with an optical apparatus that allowed us to quantify the relative sizes of the slipping and sticking regions. The ratio of the stuck skin area to the total contact area decreased linearly from 1 to 0 when the tangential force component increased from 0 to a maximum. The slope of this relationship was inversely correlated to the normal force component. The skin hydration level dramatically affected the dynamics of the contact encapsulated in the course of evolution from sticking to slipping. The specific effect was to reduce the tendency of a contact to slip, regardless of the variations of the coefficient of friction. Since grips were more unstable under dry skin conditions, our results suggest that the nervous system responds to dry skin by exaggerated grip forces that cannot be simply explained by a change in the coefficient of friction.

Keywords: skin hydration; biomechanics; biotribology; haptic; touch

1. INTRODUCTION

Human haptic behaviour depends critically on the efficient integration of afferent tactile signals. Such signals are produced by thousands of mechanoreceptors that innervate the glabrous skin and are stimulated by skin deformation [1–5]. These signals enable the central nervous system (CNS) to be aware of the properties of a touched surface, allowing the CNS to adapt its motor strategy to the intended task. See Augurelle et al. [6] and Witney et al. [7] for recent surveys. When holding an object, the normal component of the grip force must be sufficiently large to induce a tangential force component that can prevent slip [3]. The smallest grip force providing a stable grasp depends on the properties of the gripped object, including its mass, geometry, material and surface finish. Humans rely on tactile afference to adjust the grip force in accordance with such object properties [8–10]. Frictional properties and grip stability, however, also depend on skin hydration as much as they depend on the object itself [11].

Here, we experimentally investigated the details of the mechanical events occurring during the transition period between an entirely stuck contact and a fully developed slip, and the dependency of these events on skin hydration. When performing a dynamic gripping task, external loading initially deforms the skin; when slip occurs, it does so first at the periphery of the contact region according to a classic result in contact mechanics ([12], ch. 7). The time course of the strain distribution in objects in unilateral contacts that evolve from a stuck state to slip is termed 'contact dynamics' and is a branch of study of general contact mechanics. This phenomenon can be readily observed in finger slips [3,13]. The contact dynamics during the transition stage may inform the nervous system of a corrective behaviour to adopt to maintain grip stability. These transitional events, however, have not yet been directly quantified.

While many authors have considered models of finger deformation under strictly normal finger loading [14 22], composite loads that include significant tangential components are particularly relevant in the investigation of grip behaviour. Few studies have evaluated the lumped biomechanical behaviour of the fingertip. Nakazawa *et al.* [23] characterized the lumped stiffness and viscosity of the human fingertip under tangential isometric loading, and Pataky *et al.* [24] studied bulk relaxation after quasi-static loading. The micromechanical behaviour of the skin was

*Author for correspondence (jean-louis.thonnard@uclouvain.be)
Journal of the Royal Society Interface, 8(64):1574–1583, doi: 10.1098/rsif.2011.0086

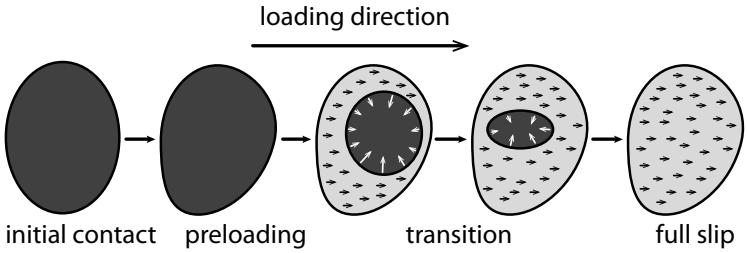

Figure 1. Course of evolution of the dynamics of finger contact from the initial contact to full slip. From left to right: initial stuck contact (dark grey), preloading, slip onset starting at the trailing edge, growth of the slip region (light grey), full slip.

studied by Wang & Hayward [25], who used miniature cantilevered benders to test the biomechanical properties of the fingerpad skin *in vivo* at a submillimetric scale. They found that the viscoelastic behaviour of the skin under local tangential loading was strongly nonlinear, and that the skin became very stiff beyond a 50 per cent strain. Significantly, these properties depended on the direction of the loading relative to the orientation of the ridges, suggesting that bulk behaviour may be difficult to predict with any level of accuracy from global simulation studies. As a result, direct observation still remains to be the most reliable method to analyse the properties of a realistic finger contact [26,27].

The conventional coefficient of friction, defined as the ratio of the tangential to normal components of a net interaction force during slip, remains a convenient abstraction, even if it depends on many exogenous and endogenous factors in a contact pair. Skin hydration is perhaps the most important of those exogenous factors, as it depends on both physiological and environmental conditions [28–32]. We previously developed an apparatus that can continuously measures skin hydration during precision gripping behaviour [33], and showed that subjects with naturally dry skin not only respond with a tighter grip to compensate for a reduced coefficient of friction, but also clearly overcompensate. This observation suggested that lumped friction was not the sole factor considered by the CNS to provide a stable grip. It could be that the nervous system is sensitive to the skin microdeformations that occur before a full slip develops, and that these micromechanical events depend strongly on skin hydration. Here, we characterized the distributed skin deformation under composite loading to assess the effect of hydration on slip onset.

A qualitative account of the transition of the course of events may be described with reference to figure 1 (see the electronic supplementary material, see also [13,26]). A gripping contact normally begins with an initial contact causing a large elliptical contact region to form. During a preloading phase, the contact is loaded tangentially causing tissue-rolling deformations that slightly modify the shape of the contact surface. If the normal component of the grip force is inadvertently too small, slip occurs, starting with the trailing edge of the contact to form a slip region that grows like bush-fire from the periphery. When it vanishes, a fully developed slip is established. We hypothesized that skin hydration affects this phenomenon through two mechanisms. Firstly, it is now known that skin friction is maximized for an optimal level of skin hydration [29]. Therefore, the transition from sticking to slip should be precipitated by a dry skin. Secondly, since a dry skin is stiffer than a well-hydrated skin [28], the critical transitional traction should be reached for small surfaces strains, causing more slip to occur for smaller net displacements.

2. METHODS

2.1. Materials

2.1.1. Optical system. We used an optical fingerprint recording technique based on the principle of frustrated total internal reflection. The apparatus included an intense diffuse light source, right-angle prism and camera (figure 2*a*). Light propagated towards the face of the prism where the fingertip was in contact. When there was no contact, light was totally reflected towards the camera, creating a bright, uniform image. When the fingerprint ridges were in contact with the prism, total internal reflection was frustrated, resulting in a high-contrast pattern of black ridges on a white background.

The optical system, originally developed by Levesque & Hayward [26], used a 250 W halogen lamp as the light source and a right-angle prism (50 × 50 × 70 mm) made of BK7 glass. A monochrome, progressive scan CCD camera (TM-6703, Pulnix America, Inc., Sunnyvale, CA, USA) recorded the reflected images with a 8-bit pixel depth and a resolution of 640 × 484 at 60 Hz. A zoom (Zoom 7000, Navitar Inc., Rochester, NY, USA) allowed the system to focus on the region of interest from a distance of 15 cm. Images were acquired in a streaming mode by a frame grabber (Meteor-II/MultiChannel, Matrox Electronic Systems Ltd., Dorval, Canada) connected to a personal computer. Images were processed using Matrox Imaging Library v. 6.1. An electronic signal generated by the frame grabber at the onset of video recording allowed synchronization with force measurements. Zoom magnification was adjusted for each subject and each normal force so that measurement resolution was maximized according to the contact surface size. After each adjustment, the system was optically calibrated using a reticule having a grid of dots 1 mm apart. The smallest measurement resolution was 20 pixels mm^{-1} in all cases.

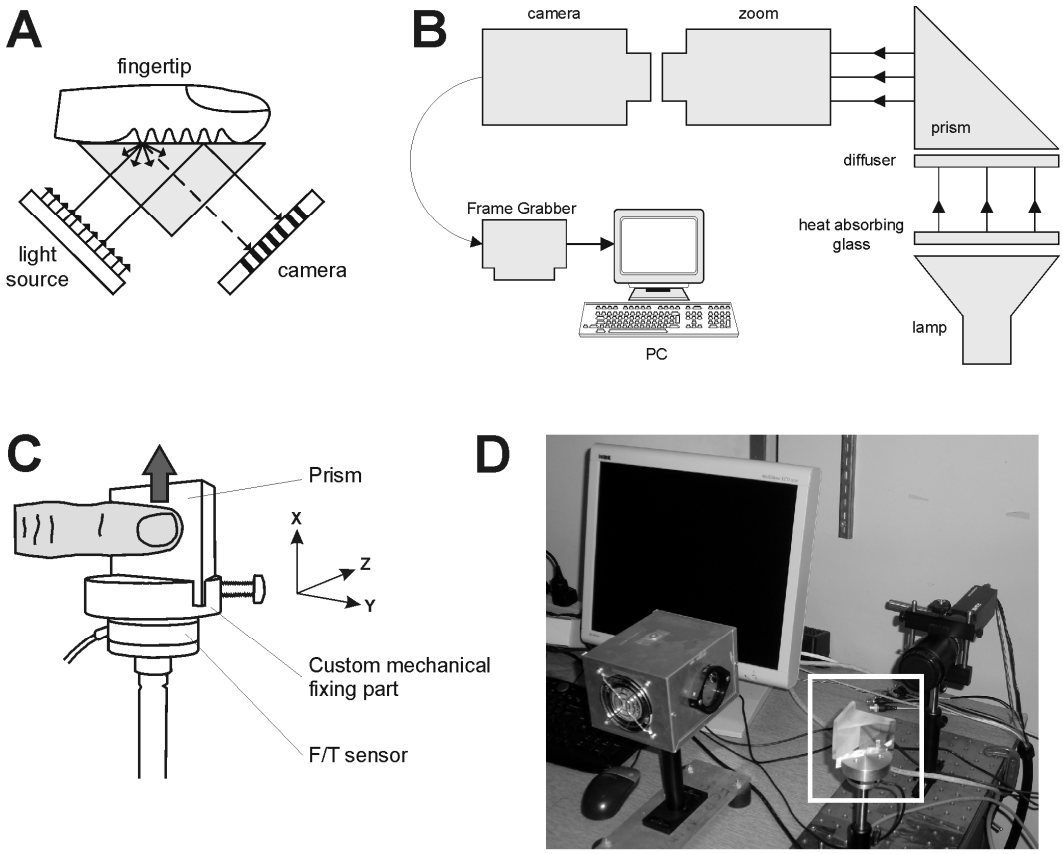

Figure 2. (*a*) Illustration of the principle of frustrated total internal reflection (FTIR) with a prism-based fingerprint imager. (*b*) Illustration of the optical platform. The light source was directed towards the prism and the camera recorded the reflected light. (*c*) Mechanical interface to record the forces applied to the prism. The task performed by the subjects is also illustrated. Subjects applied a constant normal force component and slipped in the indicated direction. (*d*) Picture of the complete system. Adapted from Lévesque & Hayward [26].

2.1.2. Mechanical system. The prism was rigidly mounted on a force/torque sensor (Mini40 F/T Transducer; ATI Industrial Automation, NC, USA) that measured the forces and torques by the subject (figure 2*c*,*d*). This set-up allowed us to determine the three components of the interaction force, F_x, F_y and F_z, in the ranges of +40, +40 and +120 N, respectively, with 0.01, 0.01 and 0.02 N resolution, respectively.

2.1.3. Skin hydration measurement. Skin hydration was measured with a Corneometer CM825, which operates using a capacitance principle. The probe comprises a 7 mm square ceramic tile with many closely spaced gold electrodes that act as capacitor plates. Electrodes are protected by a 20 μm thick vitrified dielectric material. Measurements are given in arbitrary units ranging from 20 (very dry) to 120 (very moist). The Corneometer is fully described in Fluhr *et al.* [34,35].

2.2. Experimental procedure.

Ten healthy Caucasian subjects (from 20 to 30 years of age) participated in this study. Fifteen minutes before the experiment, subjects washed their hands with soap and water and the experimenter verified that their hands were rinsed and dried carefully. All subjects provided informed consent, and the experimental protocol was approved by the local ethics committee. Subjects were seated in front of the experimental set-up and were instructed to apply a constant normal force on the imaged face of the prism with their right index fingertip. Visual feedback provided them with the normal force component actually exerted. The experimenter checked visually that the initial angle between the glass surface and their distal phalange was within 20–30°. When the normal force was stabilized at a given level (specified by the experimenter), subjects performed an ulno-radial tangential slip (vertical arrow, figure 2c). The fingertip skin moisture was measured before and after each trial. Each subject performed five trials for six levels of normal force: 0.2, 0.5, 1, 2, 5 and 10 N. Subjects easily maintained a nearly constant normal force component. Its value did not vary by more than ±10 per cent during the task.

2.3. Data processing and variables studied

The force transducer signals and the trigger signal from the CCD camera were acquired with a 12-bit 6071E analogue-to-digital converter in a PXI chassis (National Instruments, Austin, TX, USA). The trigger signal allowed synchron-

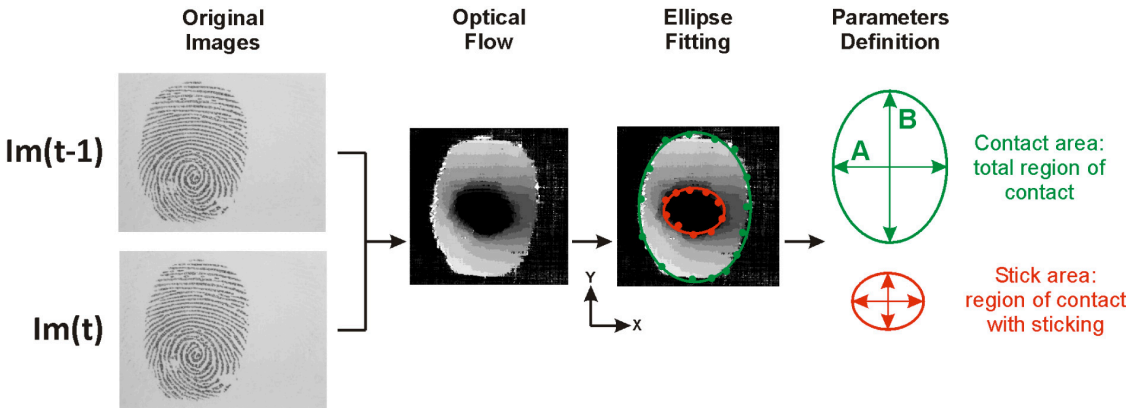

Figure 3. Image processing using the optical flow technique. By comparing two images, a gradient of displacement was estimated for each pixel. Black corresponds to zero displacement and grey levels correspond to the displacement magnitude (lighter colour indicates greater magnitude). Ellipses were fitted to quantify the contact region (green ellipse) and the stuck region (red ellipse).

ization of the video frames with the force recordings. Force signals were low-pass-filtered with a fourth-order, zero phase-lag Butterworth filter, which has a cut-off frequency of 10 Hz. Statistical analyses were performed using SAS software.

2.3.1. Image processing. Optical flow is a technique commonly used in computer vision. This technique allows the estimation of a displacement vector for each pixel of the original image, and the registration of the two images into the same coordinate system. The simplest implementation involves overlaying two or more frames taken at different instants in time [36]. We compared each selected frame of the fingertip surface of contact ($\mathrm{Im}(t_2)$, figure 3) with the previous frame ($\mathrm{Im}(t_1)$, figure 3). The displacement vector was coded using a grey scale, where black indicated a null displacement and white indicated a displacement of 20 pixels. The optical flow computation revealed a contact region represented by a grey region on a black background, and a stuck region was represented by a black region within a grey region (figure 3). Inside the contact region, the grey levels indicated the displacement gradient.

The Lucas-Kanade method [37] was used to quantify displacement. Given images $F_1(\boldsymbol{x})$ at time t_1 and $F_2(\boldsymbol{x})$ at time t_2, we sought vector $\boldsymbol{h}$, such that $F_2(\boldsymbol{x}) = F1(\boldsymbol{x}+\boldsymbol{h})$:

$$\boldsymbol{h} \approx \left[\sum_{\boldsymbol{x}} \left(\frac{\partial F_1}{\partial \boldsymbol{x}}\right)^{\top} [F_2(\boldsymbol{x}) - F_1(\boldsymbol{x})]\right] \times \left[\sum_{\boldsymbol{x}} \left(\frac{\partial F_1}{\partial \boldsymbol{x}}\right)^{\top} \left(\frac{\partial F_1}{\partial \boldsymbol{x}}\right)\right],$$

where

$$\frac{\partial}{\partial \boldsymbol{x}} = \left[\frac{\partial}{\partial x} \; \frac{\partial}{\partial y}\right]^{\top}$$

in two-dimensional images. While vector $\boldsymbol{h}$ corresponds to the global displacement between two images, the displacement can also be estimated for any portion of an image.

2.3.2. Fitting ellipses. Further characterization of the different regions was done by fitting an ellipse at the outer border of each region. This procedure provided spatial filtering that attenuated measurement noise. It also had the benefit to furnish a notion of shape for the surfaces of interest. The experimenter selected at least 10 points at the border of the region to be quantified. The best-fitting ellipse was found using a least-squares criterion that minimized the sum of the distances between the 10 points and the curve (figure 3, ellipse fitting). Considering the ellipse equation:

$$ax^2 + bxy + cy^2 + dx + ey + f = 0,$$

and letting $p = (a, b, c, d, e)$ be the vector of parameters to be estimated normalized to f, then

$$P = \frac{\sum X}{X^{\top} X},$$

where X is a matrix of the form $(x^2\, xy\, y^2\, xy)^{\top}$ of all the measurement vectors $(xy)^{\top}$. We used this procedure to estimate the areas of the total and stuck contact regions. The areas estimated with this method never differed by more than 4 per cent from the areas estimated by the time-consuming procedure of direct counting of the pixels (criterion validated on ten samples).

3. RESULTS

The temporal evolutions of the normal (NF) and tangential (TF) components of the interaction force for a typical trial are shown in figure 4 (top). When NF applied to the prism by the index finger was stabilized around the target value, subjects ramped up TF during the preloading period (figure 4, grey area) until slip fully occurred. At this point, the frictional force balanced TF and the magnitude of TF plateaued (figure 4, black arrow). During the preloading and slipping phases, a subset of frames separated by 150 ms intervals was selected to compute 'optical flow images' (figure 4, bottom; see §2.3.1). Four of these frames are exemplified in figure 4 (middle). Each of these frames was

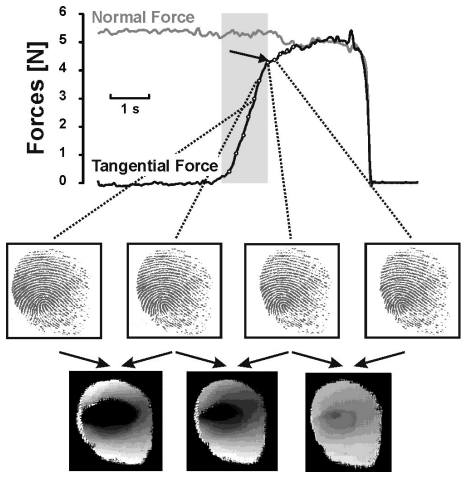

Figure 4. Time course of the normal and tangential force components in a typical trial, associated frames and 'optical flow images'. During the tangential preloading period (grey box), the tangential force component increased until the slip occurred (black arrow, top). Frames were selected during the preloading phase and were compared to obtain the optical flow images. The contact area is not correlated to the tangential force. The stuck area decreased when the tangential force component increased.

then associated to the normal and tangential force components, TF and NF, respectively (figure 4, dashed lines and white dots). The area of the contact region varied a little during the tangential loading period, while the area of the stuck region decreased significantly when TF increased. When slip was fully developed, as evidenced by optical flow processing (figure 4, bottom right), the variation of TF was quite small (figure 4, top, black arrow).

3.1. Static characteristics of the contact area

The areas of the total contact region and stuck region were estimated for each optical flow image. The subjects had large anatomical differences, as the contact areas for each subject and for a 10 N normal force varied from 177 to 288 mm2 (table 1). To compare the results between subjects, the contact region areas were normalized to the largest contact area attained when NF was 10 N. Figure 5*a* shows the relationship between NF and the normalized contact area when TF was zero. The normalized contact area increased but reached a maximal value asymptotically. At 2 N, the contact surface was nearly 80 per cent of its final value, and the contact area at 10 N was three times larger than that at 0.2 N. Thus, the contact area was sensitive to changes in NF at low values only, and was saturated at high values.

A typical time course of the normalized contact area for subject TA at a constant NF of 5 N is shown in figure 5*b* (black dots). The normalized contact area decreased moderately over time until it reached a constant value, which corresponded to the normalized contact during full slip. Because of the initial deformation of the tissues, the contact area diminished during the preloading period (grey area in figure 4). This effect translated into an average of 12.5 per cent shortening of the ellipse A-axis. During steady slip, there was very little variation in the contact area.

Table 1. Contact area of each subject when the normal force was 10 N.

subjects	contact area at 10 N (mm^2)
AC	224
AG	249
FH	228
GC	263
GT	177
MZ	183
RW	253
TA	288
VL	275
VM	251

3.2. Lumped dynamics of the contact

Figure 5*b* shows the time course of the normalized stick area (grey dots and line). During the preloading phase (grey zone, figure 4, top) when TF increased, the area of the stuck region decreased linearly until it reached zero (figure 5*b*), at which point full slip occurred. As it is a fundamental property of friction that adhesive forces are smaller than friction forces once the transient regime has settled, the measured interaction force must correlate with the ratio, SR, of the areas of the stuck region and the contact region:

$$\mathrm{SR} = \frac{\text{stuck area}}{\text{contact area}},$$

this quantity, termed the stick ratio, which varies from 1 (unloaded contact) to 0 (fully slipping contact). We averaged SR and hydration levels from five consecutive trials for each subject and for each value of NF. Interestingly, the hydration level did not vary significantly over the five trials (standard deviation = 5 arb. units).

Since SR captures the contact state in a single number, one can relate the contact state to TF (figure 6). Figure 6a,b displays the results from two subjects with obvious skin differences for NF values of 0.5 N and 5.0 N. Subject AG (green trace) had dry skin (mean hydration = 49 arb. units), while subject GC (blue trace) had moist skin (mean hydration = 110 arb. units). The lowest TF magnitudes were not correlated to SR. However, with higher TF magnitudes, SR decreased almost linearly with TF, and the negative slopes were significantly different when comparing two extreme values of hydration, especially at low NF values. This effect was quantified by computing the linear regression that fit the data for $\mathrm{SR} < 0.8$. Table 2 shows the mean slope across all subjects for different NF values. The results confirm the strong influence of the normal contact loading.

3.3. Effect of hydration

The effect of skin hydration on the finger contact dynamics can also be evaluated by comparing the relative increase in TF before slippage. Figure 6 shows with black squares the TF magnitudes for an SR of 0.5. Hydration levels could then be associated to the TF during full slip, i.e. SR = 0 (figure 6*a,b*, black circles). The ratio between the tangential force component, TF and its ultimate value, TFslip, can be viewed as a measure of the 'sensitivity' of a contact to perturbations. A 'robust' grip has a low sensitivity.

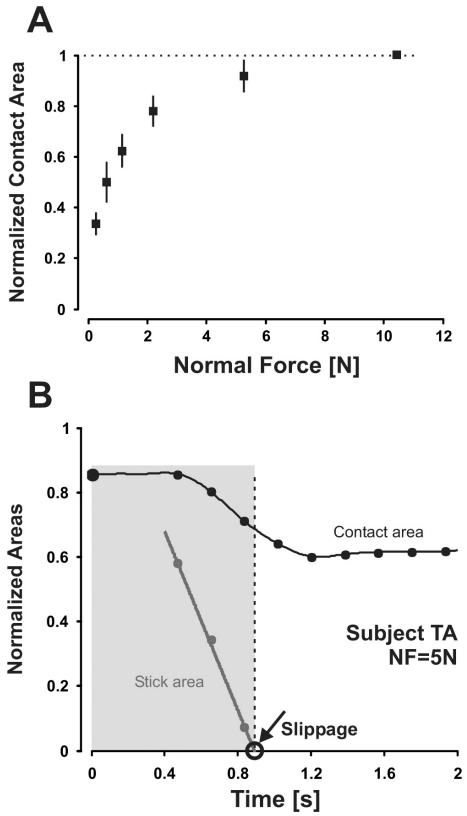

Figure 5. (*a*) Normalized contact area increased logarithmically with the normal force component. The normalized contact area was defined as the ratio between the contact area and the contact area for a normal force of 10 N. Each data point corresponds to the mean normalized contact area across all subjects. Standard deviations (vertical lines) are plotted around the corresponding means. (*b*) Typical trial showing the time course of the normalized contact area (black dots and curve) and the normalized stick area (grey dots and curve) for one subject applying a normal force component of 5 N. When the stuck area vanishes, the slip is fully developed (circle and dashed line). The grey box corresponds to the tangential preloading phase.

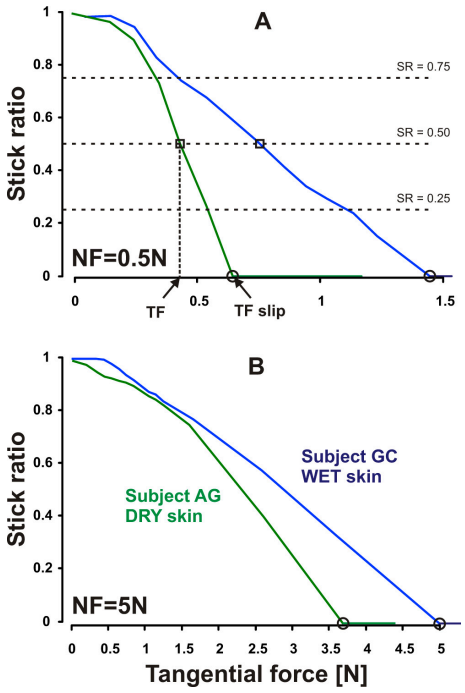

Figure 6. Relationship between the stick ratio and the tangential force for two subjects with very different hydration levels (green or blue curves) and for two normal forces (a) 0.5 N and (b) 5 N. Each curve corresponds to the mean of five trials for a given subject and a given normal force. (a) The horizontal dashed lines underline three stick ratio values (SR 14 0.25, 0.5 or 0.75). The tangential force component is found where the lines cross the curves (e.g. for SR 14 0.5, black squares). The tangential force component when the full slip occurs is found when the stick ratio is 0 (black circles). (b) Colours are associated with subjects: green trace for subject AG who had the driest skin and blue trace for subject GC who had the wettest skin.

Table 2. Mean value (± s.d.) of the slope of the linear relationship between tangential force and stick ratio, for each level of normal force across all subjects.

normal force (N)	slope
0.2	-1.81 ± 0.47
0.5	-1.29 ± 0.43
1	-0.85 ± 0.27
2	-0.44 ± 0.12
5	-0.31 ± 0.10
10	-0.19 ± 0.06

Figure 7 illustrates the effect of hydration on the quantity TF/TFslip at a specific point of a developing slip (SR = 0.5). The data are from the two subjects who exhibited the largest hydration variation for all NF values combined with a significant decrease of the ratio TF/TFslip when hydration increased ($p < 0.0051$, Bonferonni-corrected). The other subjects had an individual hydration variation below 30 arb. units. Figure 8 summarizes the data of all subjects and all NF values. Figure 8*a* shows the effect of hydration on the value of TF/TFslip for each subject for the same slip ratio value, SR = 0.5. Figure 8*b* shows the effect of hydration on the value of TF/TFslip at different phases of a developing slip (SR = 0.25, 0.5 and 0.75). On average, the ratio TF/TFslip increased as the slip ratio, SR, decreased, that is, the sensitivity of the contact decreased when it was closer to full slip. The quantity TF/TFslip also decreased with hydration for all three SR values. In other words, dry skin always corresponded to grips that were more sensitive to disturbances. The variations of TF/TFslip could be represented by a linear mixed model that used hydration as a fixed effect and the subject as a random effect (SAS software). This method allowed us to study the interaction effect between hydration and subject (hydration × subject). The results showed that hydration had a significant effect ($p < 0.001$) which was not the case of that of hydration × subject interaction ($p < 0.9706$), confirming that the effect illustrated by figure 8 is linked to hydration. The subject effect was also significant ($p < 0.001$). For a dry skin,

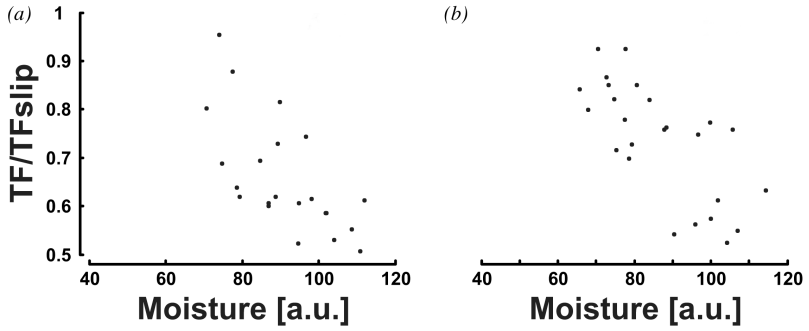

Figure 7. Effect of moisture on the ratio TF/TFslip for the two subjects (*a*) AC and (*b*) FH with the largest moisture variation. All normal forces are represented and each data point corresponds to the ratio of TF/TFslip and moisture level for one trial and for a given stick ratio (SR = 0.5).

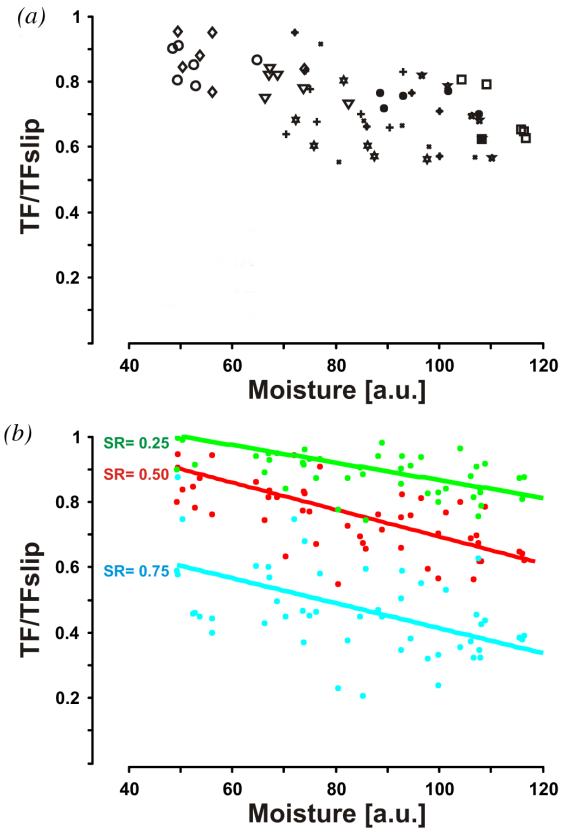

Figure 8. Effect of moisture on the ratio TF/TFslip: (*a*) with a different symbol and/or colour for each subject (SR = 0.5; AC, green circles; AG, black crosses; FH, black squares; GC, grey plus symbols; GT, green diamonds; MZ, blue inverted triangles; RW, blue stars; TA, purple stars; VL, red dots; VM, red plus symbols) and (*b*) for three stick ratio values (SR = 0.25 in green, SR = 0.50 in red and SR = 0.75 in blue). All subjects and all normal forces are represented. Each data point corresponds to the mean ratio TF/TFslip and moisture level for one normal force component value across the five trials and for a given stick ratio.

when the contact is half slipping (SR = 0.5), the ratio TF/TFslip is close to 0.9, that is, the transition to full slip is imminent. In contrast, for a higher level of hydration, this ratio can reach 0.6 for the same contact condition. Thus, when hydration is low, a 10 per cent disturbance in tangential loading can provoke slip, whereas a 40 per cent increase is needed to achieve the same result in well-hydrated skin. At any point of a developing slip, the higher the skin hydration is, the further the skin is from the full slip. This observation holds true regardless of the NF value.

4. DISCUSSION

Previous studies investigated the effects of skin hydration on the global characteristics of a finger contact [30,38–40]. The present study showed that skin hydration impacts finger contact dynamics as expressed by skin surface deformation under tangential loading. The effects of skin hydration were imaged directly and we could observe how the contact transition from adhesion to slip varied as a function of skin hydration. To quantify this effect, we first evaluated the skin area undergoing slip relative to the total contact region. We observed that the tangential force component TF reached a maximum when the entire contact surface slipped. More significantly, skin hydration strongly impacted the relative increment of tangential loading available before a complete slip developed, regardless of the normal force component NF and regardless of the contact state. In all cases, the greater the skin hydration magnitude was, the further the contact was from slipping.

4.1. The notion of incipient slip

Johansson & Westling [3] described the importance of the cutaneous sensory feedback in precision grips. They showed that the nervous system adapts the grip force as a function of object friction properties. They hypothesized that continuous tactile feedback arises from partial slips, termed 'incipient slip', occurring at the periphery of the contact region. However, few studies have quantified this effect. Tada et al. [13] introduced the SR to quantify the contact state, and presented experimental data that were similar to ours: the SR decreased linearly when tangential loading increased. However, these authors tested proximo-distal finger movements with normal force components $\leq$ 1.5 N, and did not investigate the role of skin

hydration. In the present study, we used ulno-radial movements that are more relevant to gripping behaviours, a much larger force range from 1 N to 5 N, and measured skin hydration. These factors are all significant to dextrous manipulation.

Incipient slips are widely used in robotics to develop robots that can dynamically adapt the grasp force to object properties [41–44]. Tremblay & Cutkosky [44] made a robotic finger that had an artificial skin covered with 'nibs' that formed local contact regions and could slip independently. When partial slip occurred, some 'nibs' located peripherally emitted a vibration that was used to adapt the gripping force. Maeno et al. [42] described an artificial skin with strain gauges bonded to phosphor bronze plates embedded in silicon rubber. Incipient slip was detected from the relative displacement of each plate. They showed that broad contact conditions (non-contact, slip or stick) varied with the normal and tangential force components. Recently, Edin et al. [41] developed an artificial tactile system with miniature strain gauges embedded in a biomechatronic hand that provides rich information during manipulation tasks, including slip information between the fingertip and an object.

4.2. The effect of hydration

For equivalent contact states (encoded by SR), we found that the contact safety margin increased when skin hydration increased (at least when touching a glass surface), regardless of the normal loading. This result contributes to our understanding of motor behaviour when grasping or manipulating objects. Smith *et al.* [45] observed that people who were administered scopolamine spontaneously employ higher grip forces. Scopolamine reduces skin hydration through reduced sweat gland activity, which in turn modifies the finger/object frictional interaction. Recently, we demonstrated a causal relationship between skin hydration and grip force [11]. Subjects with a dry skin spontaneously employed a greater grip force at a level that is not compatible with a simple compensation for the reduction of friction: a 40 per cent of friction reduction was associated with a 140 per cent increase of grip force. The minimal grip force required to prevent the object from slipping directly depends on the finger-object friction but the excess of grip force is also related to other factors like cognitive or environmental factors. In the light of the present results, we can speculate that the CNS behaves in such a manner that when the skin is dry, the gripping force is commanded to be exaggeratedly large to reduce the effects of disturbances. Seen from the view point of the time course of the motor commands needed to produce a stable grip, dry skin reduces the 'time-to-slip', making the grip potentially even less robust against unknown factors. The quantity TF/TFslip is analogous to the notion of the ratio of required friction to available friction that was employed in the study of Hanson et al. [46]. Interestingly, our results are also related to the findings of Gerhardt *et al.* [47], who reported to have found a linear relationship between skin hydration and skin friction. The linear decrease of the ratio TF/TFslip as a function of hydration observed in the present study could be owing to this relationship.

4.3. Tribology of finger contact and possible mechanisms

The tribology of finger skin adhering or sliding on surfaces is a complex phenomenon resulting from the interplay of several physical effects, including water-mediated capillary adhesion, plasticization of stratum corneum, ridge squashing, elastohydrodynamic lubrication and modulation of water migration as a function to the porosity of the surface in contact with the finger. All of these effects depend critically on the hydrophilic properties of the tissues of the fingertip as well as on the mechanisms of sweat secretion and re-absorbtion [28]. The combination of these effects points to a critical role of water above and beyond the modification of the frictional properties of the skin per se, having an impact on the dynamics of transition from adhesion to slip.

It is possible to speculate on the mechanisms contributing to the global effect we observed. There are at least three distinct yet related phenomena. First, moist skin is more flexible than dry skin [28]. As a result, the bulk dynamics of deformation are faster with dry skin, making it harder for the nervous system to sense them for corrective action. Second, hydration could have mechanical consequences at the scale of the ridges. Glabrous skin ridges determine the 'effective contact area' inside a contact region [48]. A moist, softer skin could reasonably provide a larger effective contact area than dry skin for the same contact region, increasing the net friction [49]. Third, the superficial, keratin-based, fibrous skin layers present strong affinity for endogenous or exogenous water, modifying the skin mechanical behaviour at the microscopic scale. Interfacial microscopic stress distributions are probably strongly dependent on the presence or absence of water, especially during interactions with smooth surfaces [50].

4.4. Perspectives

The experiment presented here was performed using active touch. Subjects exerted a force with their index finger and used visual feedback to regulate the normal component. They performed the task adequately, leading to a standard deviation of the normal component that was smaller than 20 per cent of the mean, even during the preloading phase. The spontaneous preloading period was nearly constant (approx. 700 ms) suggesting another type of compensating motor behaviour. To control these factors, in future studies, the subjects' fingers should be stimulated by a servo-controlled apparatus where all the mechanical variables could be regulated independently, including the slip velocity. Nevertheless, the mechanics of interaction should be studied together with spontaneous, task-oriented motor behaviour.

4.5. Conclusion

Skin hydration modifies the skin deformation dynamics during grip-like contacts. Certain motor behaviours observed during object manipulation could be explained by the effects of skin hydration. We suggest that the overcompensation strategy seen when the skin is dry could be explained by important variations in the contact dynamics as a function of skin hydration. Our results, so far, are specific

to glass surfaces that are perfectly smooth and stiff in the range of forces considered. The fact that glassy surfaces are not porous and confine water at the interfaces is likely to contribute to the effect that we have observed. With other contact imaging modalities, similar experiments could be conducted with surfaces such as wood or plastic. We expect that the qualitative aspects of our study would extend to these cases as well.

We are grateful to our subjects for their participation in this experiment. We extend special thanks to the Haptic Laboratory (McGill) for their warm welcome and help. This work was supported by the Fonds National de la Recherche Scientifique, the Fondation pour la Recherche Scientifique Médicale, the Belgian Program on Interuniversity Attraction Poles initiated by the Belgian Federal Science Policy Office, Actions de Recherche Concertées (French Community, Belgium), an internal research grant (Fonds Spéciaux de Recherche) of the Université catholique de Louvain, a grant from Prodex (contract nos. 90063, 90064, 90231, 90232), the ESA (European Space Agency) and the NANOBIOTACT project (EU-FPG-NMP-033287). This work was also supported by the European Research Council (FP7 Programme) ERC Grant agreement no. 247300 (to V.H.).

REFERENCES

1 Johansson, R. S. & Flanagan, J. R. 2009 Coding and use of tactile signals from the fingertips in object manipulation tasks. Nat. Rev. Neurosci. **10**, 345–359. (doi:10.1038/nrn2621)

2 Johansson, R. S. & Vallbo, A. B. 1983 Tactile sensory coding in the glabrous skin of the human hand. Trends Neurosci. **6**, 27–32. (doi:10.1016/0166-2236(83)90011-5)

3 Johansson, R. S. & Westling, G. 1984 Roles of glabrous skin receptors and sensorimotor memory in automatic control of precision grip when lifting rougher or more slippery objects. Exp. Brain Res. **56**, 550–564. (doi:10.1007/ BF00237997)

4 Johnson, K. O. 2001 The roles and functions of cutaneous mechanoreceptors. Curr. Opin. Neurobiol. **11**, 455–461. (doi:10.1016/S0959-4388(00)00234-8)

5 Srinivasan, M. A., Whitehouse, J. M. & LaMotte, R. H. 1990 Tactile detection of slip: surface microgeometry and peripheral neural codes. J. Neurophysiol. **63**, 1323–1332.

6 Augurelle, A. S., Smith, A. M., Lejeune, T. & Thonnard, J. L. 2003 Importance of cutaneous feedback in maintaining a secure grip during manipulation of hand-held objects. J. Neurophysiol. **89**, 665–671. (doi:10.1152/jn.00249.2002)

7 Witney, A. G., Wing, A., Thonnard, J. L. & Smith, A. M. 2004 The cutaneous contribution to adaptive precision grip. Trends Neurosci. **27**, 637–643. (doi:10.1016/j.tins. 2004.08.006)

8 Cadoret, G. & Smith, A. M. 1996 Friction, not texture, dictates grip forces used during object manipulation. J. Neurophysiol. **75**, 1963–1969.

9 Flanagan, J. R., Wing, A. M., Allison, S. & Spenceley, A. 1995 Effects of surface texture on weight perception when lifting objects with a precision grip. Percept. Psychophys. 57, 282–290. (doi:10.3758/BF03213054)

10 Westling, G. & Johansson, R. S. 1984 Factors influencing the force control during precision grip. Exp. Brain Res. **53**, 277–284. (doi:10.1007/BF00238156)

11 André, T., Lefèvre, P. & Thonnard, J.L. 2010 Fingertip moisture is optimally modulated during object manipulation. J. Neurophysiol. **103**, 402–408. (doi:10.1152/jn.00901.2009)

12 Johnson, K. 1985 Contact mechanics. Cambridge, UK: Cambridge University Press.

13 Tada, M., Mochimaru, M. & Kanade, T. 2006 How does a fingertip slip?visualizing partial slippage for modeling of contact mechanics. Proc. Eurohaptics 2006, Paris, France, July 2006, pp. 415–420.

14 Cohen, J. C., Makous, J. C. & Bolanowski, S. J. 1999 Under which conditions do the skin and probe decouple during sinusoidal vibrations? Exp. Brain Res. **129**, 211–217. (doi:10.1007/s002210050891)

15 Fung, Y. 1993 Biomechanics: mechanical properties of living tissue, 2nd edn. New York, NY: Springer.

16 Kim, I., Ohtsuka, H. & Inooka, H. 1994 Impedance model for human fingertips. SICE **30**, 112–114.

17 Kinoshita, G. & Mori, M. 1972 An elastic model of the skin and some properties on the variable threshold processing of an artificial tactile sense. Trans. Soc. Instrum. Control Eng. **8**, 398–405.

18 Maeno, T., Kobayashi, K. & Yamazaki, N. 1998 Relationship between the structure of human finger tissue and the location of tactile receptors. JSME Int. J. C Mech. Syst. Mach. Elem. Manuf. **41**, 94–100.

19 Pawluk, D. T. & Howe, R. D. 1999 Dynamic contact of the human fingerpad against a flat surface. J. Biomech. Eng. **121**, 605–611. (doi:10.1115/1.2800860)

20 Phillips, J. R. & Johnson, K. O. 1981 Tactile spatial resolution. III. A continuum mechanics model of skin predicting mechanoreceptor responses to bars, edges, and gratings. J. Neurophysiol. **46**, 1204–1225.

21 Srinivasan, M. A. & Dandekar, K. 1996 An investigation of the mechanics of tactile sense using two-dimensional models of the primate fingertip. J. Biomech. Eng. Trans. ASME **118**, 48–55. (doi:10.1115/1.2795945)

22 Srinivasan, M. A., Gulati, R. & Dandekar, K. 1992 In vivo compressibility of the human fingertip. Am. Soc. Mechanical Engineers, BED **22**, 573–576.

23 Nakazawa, N., Ikeura, R. & Inooka, H. 2000 Characteristics of human fingertips in the shearing direction. Biol. Cybern. **82**, 207–214. (doi:10.1007/s004220050020)

24 Pataky, T. C., Latash, M. L. & Zatsiorsky, V. M. 2005 Viscoelastic response of the finger pad to incremental tangential displacements. J. Biomech. **38**, 1441–1449. (doi:10.1016/j.jbiomech.2004.07.004)

25 Wang, Q. & Hayward, V. 2007 In vivo biomechanics of the fingerpad skin under local tangential traction. J. Biomech. **40**, 851–860. (doi:10.1016/j.jbiomech.2006.03.004)

26 Levesque, V. & Hayward, V. 2003 Experimental evidence of lateral skin strain during tactile exploration. Proc. Eurohaptics, Dublin, Ireland, July 2003, pp. 261–275.

27 Tada, M., Imai, M. & Ogasawara, T. 2000 Development of simultaneous measurement system of incipient slip

and grip/load force. Proc. 9th IEEE Workshop on Human and Robot Interaction Communication, pp. 57–62. (doi:10.1109/ROMAN.2000.892470)

28 Adams, M. J., Briscoe, B. J. & Johnson, S. A. 2007 Friction and lubrication of human skin. Tribol. Lett. **26**, 239–253. (doi:10.1007/s11249-007-9206-0)

29 André, T., Lefèvre, P. & Thonnard, J. L. 2009 A continuous measure of fingertip friction during precision grip. J. Neurosci. Methods **179**, 224–229. (doi:10.1016/j.jneumeth.2009.01.031)

30 Derler, S., Schrade, U. & Gerhardt, L.-C. 2007 Tribology of human skin and mechanical skin equivalents in contact with textiles. Wear **263**, 1112–1116. (doi:10.1016/j.wear. 2006.11.031)

31 Nacht, S., Close, J. A., Yeung, D. & Gans, E. H. 1981 Skin friction coefficient: changes induced by skin hydration and emollient application and correlation with perceived skin feel. J. Soc. Cosmet. Chem. **32**, 55–65.

32 Naylor, P. F. 1955 The skin surface and friction. Br. J. Dermatol. **67**, 239–246. (doi:10.1111/j.1365-2133.1955.tb12729.x)

33 André, T., De Wan, M., Lefèvre, P. & Thonnard, J. L. 2008 Moisture evaluator: a direct measure of fingertip skin hydration during object manipulation. Skin Res. Technol. **14**, 385–389. (doi:10.1111/j.1600-0846.2008.00314.x)

34 Fluhr, J., Elsner, P., Berardesca, E. & Maibach, H. I. 2000 Dermatology: clinical and basic science series. pp. 249–261. Boca Raton, FL: CRC Press.

35 Fluhr, J., Gloor, M., Lazzerini, S., Kleesz, P., Grieshaber, R. & Berardesca, E. 1999 Comparative study of five-instruments measuring stratum corneum hydration (Corneometer CM 820 and CM 825, Skicon 200 Nova DPM 9003, DermaLab). Part I. In vitro. Skin Res. Technol. **5**, 161–170. (doi:10. 1111/j.1600-0846.1999.tb00126.x)

36 Zitova, B. & Flusser, J. 2003 Image registration methods: a survey. Image Vis. Comput. **21**, 977–1000. (doi:10.1016/ S0262-8856(03)00137-9)

37 Lucas, B. D. & Kanade, T. 1981 An iterative image registration technique with an application to stereo vision. In Proc. 7th Int. Joint Conf. on Artificial Intelligence, August 1981,Vancouver, Canada, pp. 674–679.

38 Seo, N. J. & Armstrong, T. J. 2009 Friction coefficients in a longitudinal direction between the finger pad and selected materials for different normal forces and curvatures. Ergonomics **52**, 609–616. (doi:10.1080/00140130802471595)

39 Soneda, T. & Nakano, K. 2010 Investigation of vibrotactile sensation of human fingerpads by observation of contact zones. Tribol. Int. **43**, 210–217. (doi:10.1016/j.triboint. 2009.05.016)

40 Tomlinson, S. E., Lewis, R. & Carré, M. J. 2007 Review of the frictional properties of finger-object contact when gripping. J. Eng. Tribol. **221**, 841–850. 13506501JET313) (doi:10.1243/

41 Edin, B. B., Ascari, L., Beccai, L., Roccella, S., Cabibihan, J. J. & Carrozza, M. C. 2008 Bio-inspired sensorization of a biomechatronic robot hand for the grasp-and-lift task. Brain Res. Bull. **75**, 785–795. (doi:10.1016/j.brainresbull.2008.01.017)

42 Maeno, T., Hiromitsu, S. & Kawai, T. 2000 Control of grasping force by detecting stick/slip distribution at the curved surface of an elastic finger. In Proc. IEEE Int. Conf. on Robotics and Automation, April 2000, San Francisco, CA, pp. 3896–3901. (doi:10.1109/ROBOT.2000.845338)

43 Tada, M., Shibata, T. & Ogasawara, T. 2002 Investigation of the touch processing model in human grasping based on the stick ratio within a fingertip contact interface. In Proc. IEEE Int. Conf. on Systems, Man and Cybernetics 5, Hammamet, Tunisia, 2002, pp. 218–223. (doi:10.1109/ ICSMC.2002.1176358)

44 Tremblay, M. R. & Cutkosky, M. R. 1993 Estimating friction using incipient slip sensing during a manipulation task. In Proc. IEEE Int. Conf. on Robotics and Automation 1,1993, Atlanta, GA, pp. 429–434. (doi:10.1109/ ROBOT.1993.292018)

45 Smith, A. M., Cadoret, G. & St-Amour, D. 1997 Scopolamine increases prehensile force during object manipulation by reducing palmar sweating and decreasing skin friction. Exp. Brain Res. **114**, 578–583. (doi:10.1007/PL00005666)

46 Hanson, J. P., Redfern, M. S. & Mazumdar, M. 1999 Predicting slips and falls considering required and available friction. Ergonomics **42**, 1619–1633. (doi:10.1080/001401399184712)

47 Gerhardt, L. C., Strassle, V., Lenz, A., Spencer, N. D. & Derler, S. 2008 Influence of epidermal hydration on the friction of human skin against textiles. J. R. Soc. Interface **5**, 1317–1328. (doi:10.1098/rsif.2008.0034)

48 Warman, P. H. & Ennos, A. R. 2009 Fingerprints are unlikely to increase the friction of primate fingerpads. J. Exp. Biol. 212, 2015–2021. (doi:10.1242/jeb.028977) Wolfram, L. J. 1983 Friction of skin. J. Soc. Cosmet. Chem. **34**, 465–476.

49 Persson, B. N. J., Sivebaeck, I. M., Samoilov, V. N., Zhao, K., Volokitin, A. I. & Zhang, Z. 2008 On the origin of Amonton's friction law. J. Phys. Condens. Matt. **20**, 395006. (doi:10.1088/0953-8984/20/39/395006)